Constraining a complex biogeochemical model for multi-site greenhouse gas emission simulations by model-data fusion

Tobias Houska[1], David Kraus[2], Ralf Kiese[2], Lutz Breuer[1,3]

[1] Institute for Landscape Ecology and Resources Management (ILR), Research Centre for BioSystems, Land Use and Nutrition (iFZ), Justus Liebig University Giessen, Giessen, 35392, Germany
[2] Institute of Meteorology and Climate Research - Atmospheric Environmental Research (IMK-IFU), Garmisch-Partenkirchen, 82467, Germany
[3] Centre for International Development and Environmental Research (ZEU), Justus Liebig University Giessen, Giessen, 35392, Germany

Correspondence to: Tobias Houska (tobias.houska@umwelt.uni-giessen.de)

Abstract. This paper presents results of a combined measurement and modelling strategy to analyse N_2O and CO_2 emissions from adjacent arable, forest and grassland sites in Germany. Measured emissions reveal seasonal patterns and management effects like fertilizer application, tillage, harvest and grazing. Measured annual N_2O fluxes are 4.5, 0.4 and 0.1 kg N ha^{-1} a^{-1}, while CO_2 fluxes are 20.0, 12.2 and 3.0 t C ha^{-1} a^{-1} for the arable, grassland and forest sites, respectively. An innovative model-data fusion concept based on multi-criteria evaluation (soil moisture in different depths, yield, CO_2 and N_2O emissions) is used to rigorously test the biogeochemical LandscapeDNDC model. The model is run in a Latin Hypercube based uncertainty analyses framework to constrain model parameter uncertainty and derive behavioral model runs. Results indicate that the model is in general capable to predict the trace gas emissions, evaluated by RMSE as an objective function. The model shows reasonable performance in simulating the ecosystems C and N balances. The model-data fusion concept helps to detect remaining model errors like missing (e.g. freeze-thaw cycling) or incomplete model processes (e.g. respiration amount after harvest). It further elucidates identifying missing model input sources (e.g. uptake of N through shallow groundwater on grassland during the vegetation period) and uncertainty in measured validation data (e.g. forest N_2O emissions in winter months). Guidance is provided to improve model structure and field measurements to further advance landscape scale model predictions.

1 Introduction

Carbon dioxide (CO_2) and nitrous oxide (N_2O) are two prominent greenhouse gases (GHG) contributing to global warming, the latter having a 300 times higher global warming potential (GWP) than CO_2 considering a 100 year time horizon (Myhre et al., 2013). Terrestrial ecosystems play an important role in the global atmospheric budgets of both GHGs (Cole et al., 1997). Global CO_2 emissions from soils are five times higher than anthropogenic (mainly fossil fuel) CO_2 emissions (Raich and Schlesinger, 1992; updated with recent fossil fuel data by Boden, et al., 2010), while agricultural land use release over 60% of the global anthropogenic N_2O emissions in 2005 (IPCC, 2007). Besides the radiative forcing of both GHGs, N_2O is currently the main driver of stratospheric ozone depletion (Ravishankara et al., 2009) causing increased ultraviolet radiation, which

could result in skin cancer and other health problems (Graedel and Crutzen, 1989). While CO_2 is exchanged with the soil (heterotrophic respiration) and the vegetation (photosynthesis and autotrophic respiration), N_2O fluxes refer mainly to nitrification and denitrification processes occurring only in the soil (Butterbach-Bahl et al., 2013).

Emissions of both GHGs are highly variable in space, time and depend on a multitude of different interacting environmental

5   factors, e.g., land use/management, nitrogen/carbon inputs, meteorological conditions and physical and chemical soil properties (Davidson, 1992; Smith et al., 2003). They are largely regulated by plant physiological (Rochette et al., 1999) and microbial processes (Burton et al., 2008). Field measurements of GHG emissions and environmental drivers have allowed a basic understanding of observed emissions patterns. Nevertheless, the large number and complexity of the processes involved in the production and consumption of CO_2 and N_2O still challenge the reliable quantification of GHG emission (Butterbach-

10   Bahl et al., 2013). Therefore, various biogeochemical models have been developed in recent years for temporal as well as spatial up-scaling of GHG emissions, hypothesis testing of our process understanding, and, moreover, for scenario analyses and evaluation of efficient mitigation options (Kim et al., 2015; Molina-Herrera et al., 2016). These include, e.g. BASFOR (Van Oijen et al., 2005), CERES-EGC (Gabrielle et al., 2006), COUP (Jansson, 2012), DAYCENT (Parton et al., 1998) or DNDC and its descendant LandscapeDNDC (Haas et al., 2013). However, models remain as simplifications of the real world,

15   driven by uncertainties due to intrinsic model structure, parameterization and the current model state (Vrugt, 2016). During model application, further uncertainties are added by applied forcing data (Kavetski et al., 2006). However, currently there is no method available dealing properly with all those sources of uncertainty at the same time (Vrugt, 2016). One promising way to reduce the magnitude of model output uncertainties is to use model-data fusion techniques, i.e. matching model prediction with multiple observations by varying model parameters or states using statistical uncertainty estimation (Keenan et al., 2011).

20   There are several statistical uncertainty estimation methods available, e.g., formal Bayesian approaches like DREAM (Vrugt, 2016) or informal Bayesian approaches like GLUE (Beven and Binley, 1992). However, they are mostly used to fit models to single types of observation (Giltrap et al., 2010). Innovative multiple observation data evaluation with model-data fusion is getting common in ecosystem carbon modelling (Wang et al., 2009) and is getting more and more important in the nitrogen modelling community, too (Wang and Chen, 2012). Gained knowledge can and should be used to guide further model

25   improvements (Vrugt, 2016).

This work focuses on establishing model-data fusion in the biogeochemical community – i.e. showing their capability to gain knowledge with process-based model application. We present weekly measurements of CO_2 and N_2O emissions from a developed landscape including different land uses, i.e., arable, grassland and forest ecosystems, covering a two years period of observations. In addition to field measurements, we set up the biogeochemical LandscapeDNDC model for each of the three

30   land uses. During model-data fusion with GLUE, we rigorously accept only model runs, which return concurrent, acceptable outputs for N_2O, CO_2, soil moisture in different depths and yields. Posterior model runs are not only evaluated fulfilling appropriate objective functions, but also regarding realistic simulations of GHG emissions for separate seasons, annual sums as well as before and after land management. The model is finally used to estimate the magnitude and uncertainty of C and N fluxes, like N_2 emissions or autotrophic and heterotrophic CO_2 emissions, which are experimentally not yet quantifiable *in*

situ. Remaining model and data errors are traced back to their potential sources to improve ongoing measurements and future model applications.

2 Material and methods

2.1 Study area

5   The study area is located in the catchment of a low-mountainous creek (Vollnkirchener Bach) in the municipality Hüttenberg, Hesse, Germany (50°29′56″ N, 8°33′2″ E). One kilometer north of the village Vollnkirchen, next to the creek, we established eight transects (oriented mostly vertical to slope) along a valley cross section covering different types of land uses (Fig. 1) for GHG emission measurements. See Table 1 for detailed information on soils characteristics. Three transects (A1-A3) are located on arable land westwards the creek and were cultivated with the same field management and crop rotations (Table 1).

10   Three transects are located in a light beech (*Fagus sylvatica*) forest (W1-W3) with young and old trees on a steep hillside (slope: 10%) eastwards the creek. A shallow 0.05 m litter layer characterizes the forest soils. Furthermore, there are two transects (G1, G2) located on grassland in 4 m distance on each side to the Vollnkirchener Bach. One of the two transects is managed and grazed (G1) and is mainly covered with brown knapweed (*Centaurea jacea*), meadow foxtail (*Alopecurus pratensis*), red clover (*Trifolium pretense*) and ribwort plantain (*Plantago lanceolate*). The second grassland transect (G2)

15   represents a wetland and is mainly covered by meadowsweet (*Filipendula ulmaria*), common nettle (*Urtica dioica*), hoary ragwort (*Senecio erucifolius*) and field bindweed (*Convolvulus arvensis*). The groundwater table is close to the surface on both grassland sites. Mean annual wet deposition of nitrate and ammonium were measured from 2013–2015 with 1.66 kg N ha^{-1} and 3.45 kg N ha^{-1}, respectively. In the catchment mean annual precipitation is 588 mm and mean annual temperature is 10.5 °C for the hydrological year 01.11.2013–31.10.2014 (Seifert et al., 2016). Soil moisture is measured at A3 [0.2, 0.4 and

20   0.6 m], at G2 [0.1 and 0.25 m] and at W1 [0.15 and 0.25 m] and recorded in hourly resolution since 2013.
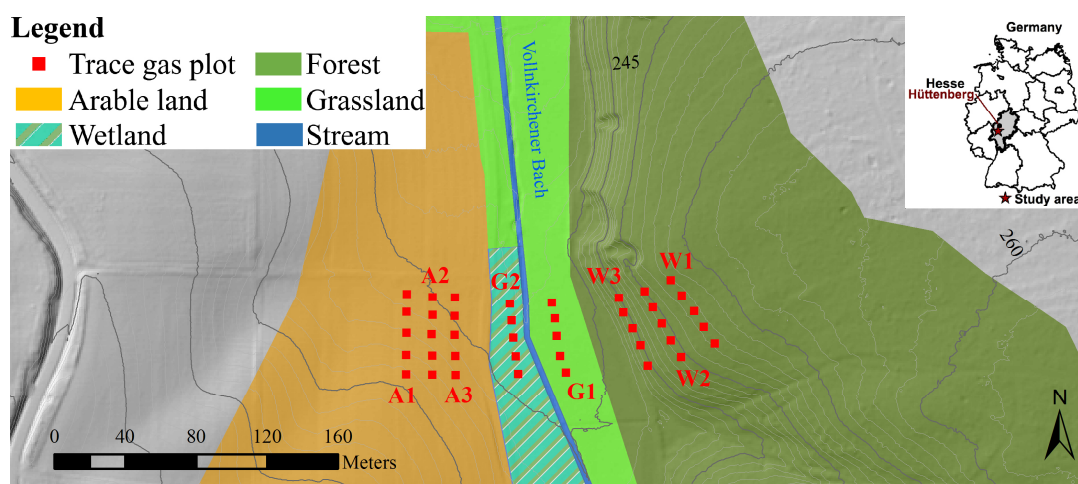
Figure 1: Map of the study area. Red squares represent GHG chamber positions at the different transects. Dark grey contour lines represent 5 m differences in elevation, light grey areas are outside of the catchment area.

2.2 Trace gas measurement

The weekly trace gas measurements started in November 2013. GHG exchange fluxes were manually measured with non-steady state opaque chambers each covering a basal area of 0.12 m². Chambers were placed on frames (both polypropylene) which were inserted approx. 8 cm into the soil in order to facilitate gas tight sampling as well as to avoid soil structure damage

5   and lateral trace gas leakage. Each chamber is equipped with an extraction septum, a counterbalance valve (in-box pressure balance) and a small fan/ventilator for homogenous mixing of the headspace air. During a 40 minutes closure period five air samples are taken from the chamber headspace at regular time intervals t0-t4 of ten minutes (0, 10, 20, 30 and 40 min.). Samples are analyzed by gas chromatography (GC 8610C, SRI Instruments, Torrance, US) with an ECD for N_2O and a methanizer and FID for CO_2. Sampling was performed on a weekly basis with five replicated chambers per transect sampled

10   by the gas sample pooling technique (Arias-Navarro et al., 2013). According to this approach, at any time interval (t0-t4) 10 ml headspace sample are collected subsequently from any of the five replicated chambers and are pooled into one gas tight glass vial (SRI Instruments). Trace gas fluxes are calculated from the rate of change in the headspace gas concentration over time by linear regression and were corrected by chamber temperature, atmospheric pressure and chamber volume according to Barton et al. (2008). All measurements with regression quality of $r^2 < 0.7$ for CO_2 (using at least four individual samples)

15   were rejected.

Soil emissions of CO_2 and N_2O can be subject to significant diurnal patterns with peak values observed in the early afternoon (Savage et al., 2014), making an up-scale process of hourly measured emissions (usually obtained at midday) to daily values difficult. We performed multiple linear regression (ordinary least square regression including air temperature, relative humidity and water filled pores space), to account for difference between, e.g., daytime (Wohlfahrt et al., 2005a) and nighttime

20   respiration (Wohlfahrt et al., 2005b). In our dataset, only CO_2 emissions showed significant correlations with mentioned environmental drivers on arable land ($r^2 = 0.53$), grassland ($r^2 = 0.59$) and forest ($r^2 = 0.51$). Following Subke et al. (2003), we derived an hourly integration formula in order to obtain daily representative mean values of CO_2 emissions from our field measurements conducted mostly between 9am–5pm. N_2O emissions are up-scaled to daily mean values with the common approach, i.e., by multiplying hourly emissions with 24. Annual CO_2 and N_2O emissions are calculated by linear interpolation

25   between the measurements. All the underlying data of chapter 2.1 and 2.2 is available on request from a database (http://fb09-pasig.umwelt.uni-giessen.de:8081/).

2.3 Modelling approach

2.3.1 Model set up

We tested the biogeochemical model framework LandscapeDNDC (Haas et al., 2013) with the observed data of our study area.

30   Individual models were set up for arable, grassland and forest ecosystems. The modules describe different processes in ecosystem compartments, i.e. mathematical descriptions of microclimate, water cycle, plant physiology and soil biogeochemical processes. We applied the biogeochemical module MeTrˣ (Kraus et al., 2015) and the watercycle module

watercycleDNDC (Kiese et al., 2011) for all land uses, but selected individual physiology modules, i.e. arableDNDC for arable, PSIM/TREEDYN for forest and grasslandDNDC for grassland simulations. As LandscapeDNDC is not yet capable for wetland simulation, we included only G1 within the modelling activities. The three different model setups were driven by the same meteorological data and initialized by land use specific soil and vegetation characteristics (Table 1).

5 **Table 1: Input settings of the LandscapeDNDC model for the three different land uses in the Vollnkirchener study region, based on measurements and farmers management documentation. In case spans are given, they reflect observed ranges for measurements used throughout the set up of the soil profile. The soil depth was estimated for model set up.**

Input	Arable (A1-3)	Grassland (G1)	Forest (W1-3)	Unit
Vegetation type	09/10–07/11 Winter Barley 08/11–08/12 Rape 10/12–08/13 Winter Wheat 10/13–08/14 Triticale 09/14–08/15 Triticale 10/15–07/16 Rape	Perennial grass	Light beech forest	-
Soil texture	Sandy clay loam	Sandy clay loam	Sandy clay loam	-
Soil type	Stagnic Luvisol	Gleysol	Cambisol	
Bulk density	1.55–1.60	1.20–1.44	1.36–1.49	g cm^{-3}
Organic carbon	1.57–0.91	2.55–0.71	3.61–1.73	%
Organic nitrogen	0.16–0.09	0.29–0.08	0.21–0.11	%
Clay content	23–26	24–25	24–26	%
pH	6.45	4.42	3.5–5.5	-
Soil depth	2.00	0.50	0.55	m

Arable soils are Stagnic Luvisols with a thick loess layer, modeled down to 2.0 m, while actual soil depth is unknown. Gleysols

10 at the meadow grassland site was modeled down to 0.5 m, which is approximately the mean annual groundwater table depth. The thin and stony soil at the forest site is a Cambisol and modeled until bedrock (0.55 m) with a litter height of 0.05 m. Bulk density is increasing for every land use in depth, while soil organic carbon and nitrogen are decreasing with depth. We run simulations for any land use in daily time resolution for 6 years, starting on 1st January 2010 with a model spin-up time of two years.

15 **2.3.2 Model-data fusion**

For the multi-objective Bayesian model calibration we used a two-tiered Generalized Likelihood Uncertainty Estimation (GLUE) approach (Beven and Binley, 1992). The model was started in both tier for 100,000 times by changing the parameter sets by Latin Hypercube sampling using the Python software SPOTPY (Houska et al., 2015). Parameters for the physiology and the water-cycle modules where treated land use-specifically, while the parameters of the biogeochemical module were

20 calibrated using data of all land uses (Table A1). We assume no prior knowledge than the given parameter ranges, i.e. consider a uniform (non-informative) prior probability distribution for all parameters. We statistically judged the performance of every parameter set to reproduce measurements with a root mean squared error (RMSE). Similar to Bloom and Williams (2015), we do not explicitly consider measurement uncertainty during model data fusion. As shown in Houska et al. (2017), one-tier

GLUE based multi-objective model calibration can result in very low acceptance rates down to 0.01%. We therefor considered a two-tiered GLUE approach, in order to increase identifiability and accuracy of accepted model runs:

Tier I: In a first step we constrained the parameter space of the hydrology and plant physiology modules of LandscapeDNDC (Table A1). We accepted only model runs, which are within the best 5% of all simulated RMSEs in terms of the respective variable (WFPS in different depths [arable in 0.2, 0.4 and 0.6 m, grassland in 0.1 and 0.25 m and forest in 0.15 and 0.25 m], as well as yield on arable land). Parameter sets were accepted, if they belong to the 5% best model runs for each land use. Results of tier I are summarized in supplement Fig. A1-A4 and are not further discussed in this paper, as they belong to the initialization of the model.

Tier II: In order to achieve realistic GHG simulations from the biogeochemical module MeTr^x of LandscapeDNDC, we took the posterior parameter boundaries of tier I and ran GLUE again. This time, we considered the best 5% of all RMSEs in terms of respective N_2O and CO_2 emissions for each land use (A1-3, G1 and W1-3). Again, only the 5% best parameter sets were accepted per land use. These results are shown in the following chapters.

Posterior model runs of tier II were further investigated in three different ways:

(1) Seasonal comparisons of measured and modeled emissions for spring (21.03-20.06.), summer (21.06.-20.09.), autumn (21.09.-20.12.), and winter (21.12.-20.03.).

(2) Management comparison of measured and modeled emissions, i.e. investigation of model performance within two weeks before and two weeks after management events to check model performance in generating hot moments, e.g. after fertilizer application.

(3) Model performance in simulating magnitude and uncertainty of C and N fluxes not measured *in situ*, like N_2 or autotrophic and heterotrophic components of CO_2 emissions.

3 Results and discussion

3.1 Measured N_2O fluxes

To determine the representativeness of each transect for a given land use, respective differences of measured N_2O emissions were compared (Table 2). Temporal dynamics of N_2O emissions are presented (Fig. 3), separated into different seasons (Fig. 4) and before/after management-events occur (Fig. 5). The mean annual N cycle is given in Table 4.

Arable N_2O fluxes: Emissions on arable land vary between 0 and 0.3 kg N_2O-N ha^{-1} day^{-1}. There were no statistical differences over time between the three arable transects. Highest emissions occur after management events. Especially mineral fertilizer application stimulates N_2O emissions, causing hot moments from e.g., March to May 2014. Input of N through manure application has a minor influence on the magnitude of N_2O emissions. Mean annual measured N_2O emissions from arable land are comparably high with 4.5 kg N_2O-N ha^{-1} a^{-1} (Jungkunst et al., 2006), equaling a GWP of 1,338 kg CO_2-C equiv. ha^{-1} a^{-1}. With yearly fertilizer application of 248.2 kg N a^{-1} a mean annual emission factor (EF) of 1.4% (varying between 1.2% for A2 and 1.8% for A3) can be calculated, where 1 kg N ha^{-1} a^{-1} is attributed to background emissions of unfertilized soil (IPCC,

1997). This EF is inside the IPCC assumed range 1.25 ±1% and close to the average EF (1.56%) of several (n=56) agricultural sites in Germany (Jungkunst et al., 2006). A robust finding throughout the literature is that reduced nitrogen input would lead to lower and therefore more climate-friendly agriculture (Bouwman et al., 2002).

Grassland N_2O fluxes: N_2O emissions vary significantly between the grazed site G1 and the wetland site G2, which can be

5   attribute to differences in management, hydrological, soil and vegetation characteristics. Most likely, nitrate supply through groundwater and uptake by the rooting system of the plants is important (Liebermann et al., 2017). Even though the groundwater table (0.2 - 0.4 m below ground) is rather shallow in winter/spring, uptake rates in summer/autumn (groundwater table 0.3 - 1.0 m below ground) are supposedly larger due to the vegetation period. Here, capillary rise might play a relevant role (Orlowski et al., 2016). While G1, with a mix of *Centaurea jacea*, *Alopercurus pratensis*, *Plantago lancelotata* and

10   *Trifolium prantense,* is grazed by sheep twice a year and cut once a year, the non-managed transect G2 is dominated by other species like *Urtica dioca*, *Filipendula ulmaria* and *Senecio erucifolius.* Typically, a deeper rooting system is found compared to G1 and accordingly, additional nitrate uptake from the groundwater is more prevalent. Mean measured emissions are higher on non-managed G2 than on grazed G1 throughout the year, especially during summer and autumn (Fig. 3). Emissions from grazed grassland vary between -0.0019 and 0.014 kg N ha^{-1} day^{-1}. High emissions were measured after grazing, e.g. in March

15   2014 when sheep dung was stimulating N_2O emissions. Negative values depict N_2O uptake, frequently found under prevailing wet conditions in spring, also reported by Glatzel and Stahr (2001). The grassland annual N_2O emissions are much lower than observed for the arable system (A1-3). However, with 0.29 (G1) and 0.52 kg N_2O-N ha^{-1} a^{-1} (G2) they are in line with a study site 12 km northeast of our site, where annual emissions amount to 0.18 to 0.79 kg N_2O-N ha^{-1} a^{-1} on an unfertilized grassland with shallow groundwater table (Kammann et al., 1998). They also report a similar seasonal pattern we found, with emissions

20   close to zero in the dry and colder autumn months. Measured annual emissions are below the assumed background level of N_2O-N emissions of 1 kg N_2O-N ha^{-1} a^{-1} from agricultural soils (IPCC, 1997). Our annual N_2O emissions equal a GWP of 87 (G1) and 156 kg CO_2-C equiv. ha^{-1} a^{-1} (G2). The EF through grazing is 5.4%, which is in line with usually found emissions factors from extensive grazed grasslands, ranging globally from 0.2 - 9.9% (Oenema et al., 1997).

Forest N_2O fluxes: Significant differences were found for the forest transects W2 and W3, which can be explained by natural

25   variations along the steep hillslope: On the hillside (W2) the soil is potentially washed out through lateral transport leading to decreased nutrition availability, compared to the dryer top (W1, +300% N_2O emissions) and the wetter hillfoot (W3, +430% N_2O emissions). N_2O emissions from the forest transects are most of the time low between -0.003 and 0.004 kg N ha^{-1} day^{-1}. Higher emissions were measured only for several weeks in January 2014, with highest values observed at W1. We contribute this to freeze thaw effects, typically found when year-around measurements are considered (Papen and Butterbach-Bahl, 1999).

30   Negative fluxes were measured e.g. in March and May 2014. The underlying process of N_2O uptake has been reported before (e.g. Flechard et al., 2005; Neftel et al., 2007) and is assumed to be a microbial process, in which denitrifier use N_2O as an electron acceptor for respiration under wet/anaerobic conditions (Bremner, 1997). Negative emissions are positively correlated with WFPS (Fig. A3) being in line with Bremner (1997). Our annual measured emissions in forest are with 0.08 kg N_2O-N ha^{-1} a^{-1} (GWP of 25 kg CO_2-C equiv. ha^{-1} a^{-1} CO_2 emissions) much lower than at adjacent grassland and arable

sites. Even more they are a magnitude lower than the N_2O emissions (5.1 kg N_2O-N ha^{-1} a^{-1}) measured from a beech forest in the Högelwald, Germany (Papen and Butterbach-Bahl, 1999). A likely reason is the substantially higher annual deposition rate of 25 kg N ha^{-1} a^{-1}, a five times higher N input as compared to our system. However, our measurements of N deposition only includes wet deposition. Additional dry depositions is often assumed to add another 30-60% to total atmospheric N deposition

5 (Flechard et al., 2011).

Table 2: Mean measured annual fluxes (11/2013-12/2015) on the different land use transects of the Vollnkirchener Bach study area. Differences between the investigated transects and land uses for measured and modeled N_2O emissions in kg N-N_2O ha^{-1} a^{-1}. * = significant difference (p < 0.05, Kruskal-Wallis test). Arable (A1-3), Grassland (G1), Wetland (G2), Forest (W1-3), RMSE in
10 **kg N-N_2O ha^{-1} day^{-1}.**

	A1	A2	A3	G1	G2	W1	W2	Measured	Mean measured	Mean simulated	Posterior RMSE
A1								4.08			0.0326 - 0.0353
A2								3.87	4.49	7.33	0.0238 - 0.0278
A3								5.53			0.0285 - 0.0329
G1	*	*	*					0.29	0.29	0.69	0.0029 - 0.0038
G2	*	*	*	*				0.52			not simulated
W1	*	*	*		*			0.09			0.0022 - 0.0025
W2	*	*	*	*	*			0.03	0.08	0.33	0.0014 - 0.0021
W3	*	*	*		*		*	0.13			0.0018 - 0.0021

3.2 Measured CO_2 fluxes

Emissions measured using our closed chamber on arable and grassland include those from soil and vegetation as the entire plants are covered by the chamber. Therefore, we interpret these emissions as total ecosystem respiration (TER). In contrast,
15 chambers in the forest were placed on the forest floor without any vegetation inside, thus, these measurements include soil (heterotroph) and root (autotroph) respiration, only. For the sake of a better read-flow, we decide to define emissions from the different land use as 'CO_2 emissions', even though we considered the different flux components on different land use. To determine the representativeness of each transect for a given land use, respective differences of measured CO_2 emissions were compared to each other (Table 3). Measured CO_2 emissions are given in time (Fig. 6), separated into different seasons (Fig. 7)
20 and before/after management-events occur (Fig. 8). The mean annual N cycle is given in Table 5.

Arable CO_2 fluxes: Weekly measured values from our arable transects range between 0 and 199.6 kg C-CO_2 ha^{-1} day^{-1} and are not significantly different. Emissions occur mainly during the growing season, starting in March and ending in November. For a comparable study site in southern Finland, reported daily TER values under barley during May and September were between 23.6 to 235.6 kg C-CO_2 ha^{-1} day^{-1} (Lohila et al., 2003), which is in the same range as our observations. The annual sum of our
25 TER emissions is 19.96 t C-CO_2 ha^{-1} a^{-1}. This is slightly lower than yearly TER measured on a winter wheat study site in Belgium with 23.18 t C-CO_2 ha^{-1} a^{-1} (Suleau et al., 2011). Demyan et al. (2016) reported lower values with an average sum of 11.43 t C-CO_2 ha^{-1} a^{-1}, derived from observations spanning six growing seasons in southwest Germany. However, all studies are possibly prone to overestimations of the emissions from September to November, as daily emissions are generated with a

multiple linear regression, in our case based on our hourly measurements of air temperature and soil moisture. Such methods do not fully account for management effects like harvest (Subke et al., 2003).

Grassland CO_2 fluxes: Emissions from grassland vary from 5.0 to 68.3 (G1) and from 0 to 92 kg C-CO_2 ha^{-1} day^{-1} (G2), with no significant difference between the two transects. Emissions are close to zero in the winter months (December to February) and highest during the growing season. A distinct negative correlation of measured CO_2 fluxes was found during wet conditions from end of June to July in 2014. In this time emissions drop to values of 41.0 kg C-CO_2 ha^{-1} day^{-1}. The TER of a grassland CO_2 is mainly driven by the growing season (Soussana et al., 2007). Emissions typically end with pasture growth during temperatures under 5°C (Parsons, 1988). Total yearly emissions are 11.79 t C-CO_2 ha^{-1} a^{-1}, which agrees well with mean yearly emissions reported for 19 different grassland sites across Europe with mean annual emissions of 12.83 t C-CO_2 ha^{-1} a^{-1} (Gilmanov et al., 2007). However, due to the many different grassland sites considered in their study, Gilmanov et al. report a much wider range of observed annual TER values from 4.9 to 16.4 t C-CO_2 ha^{-1} a^{-1}. They also found that management as a main influence on TER, where intensively managed grassland produce higher emissions than extensively managed grasslands. With regard to grazing, we found only a minor direct impact on measured flux rates (Fig. 7).

Forest CO_2 fluxes: Mean measured soil respiration span from 2.1 to 19.9 kg C-CO_2 ha^{-1} day^{-1}. While we found higher emissions in the summer months, seasonal differences have a lower magnitude as TER on arable and grassland. This was expected, as we do not measure above ground biomass respiration on our forest study site. Overall, rewetting has the strongest influence on changes of soil respiration in our forest study sites. Highest emissions occur in July 2014 after several rewetting events of the uppermost soil layer (Fig. A1). Xiang et al. (2008) reported that multiple rewetting led up to eight-times higher respiration rates. Total yearly soil emissions are with 2.98 t C-CO_2 ha^{-1} a^{-1} at the lower end of other European forest ecosystems, e.g. 6.6 ± 2.9 t C-CO_2 ha^{-1} a^{-1} as reported by Janssens et al., (2001). The uphill transect W1 has the highest emission rates throughout the year and shows significant differences to W2 and W3. This transect is less shaded through trees, resulting in a 1.3°C higher annual mean soil temperature compared to W2 and W3, likely causing higher CO_2-emissions (Table 3).

Table 3: Mean measured annual fluxes (11/2013-12/2015) on the different land use transects of the Vollnkirchener Bach study area. Differences between the investigated transects and land uses for measured and modeled CO$_2$ emissions in t C-CO$_2$ ha^{-1} a^{-1}. * = significant difference (p < 0.05, Kruskal-Wallis test). Arable (A1-3), Grassland (G1), Wetland (G2), Forest (W1-3) , RMSE in kg C-CO$_2$ ha^{-1} day^{-1}.

	A1	A2	A3	G1	G2	W1	W2	Measured	Mean measured	Mean simulated	Posterior RMSE
A1								20.10			30.73 - 36.38
A2								22.25	19.96	20.53	35.66 - 42.26
A3								17.54			22.90 - 28.46
G1								11.79	12.17	13.24	7.01 - 9.08
G2								12.54			
W1	*	*	*	*	*			4.00			3.53 - 3.89
W2	*	*	*	*	*	*		2.38	2.98	3.28	3.37 - 4.07
W3	*	*	*	*	*	*		2.56			3.15 - 3.96

3.3 Modeled N fluxes

After selecting the posterior model runs according to chapter 2.3.2, we found the model generally capable in reproducing the measured data and consequently investigate the modeled C and N cycle in more detail. Modeled N$_2$O emissions are shown for the different land use over time (Fig. 2), separated into different seasons (Fig. 3) and before/after management-events occur (Fig. 4). The complete modeled N cycle is given in Table 4.

Arable N cycle: Arable simulations consider an annual N input of 198 kg N ha^{-1} a^{-1}. This input is balanced by 109 kg N ha^{-1} a^{-1} gaseous (primarily N$_2$), 30 kg N ha^{-1} a^{-1} nitrate leaching and 99 kg N ha^{-1} a^{-1} harvest losses (Table 4), meaning that modeled outputs are higher as the given inputs. This gap in the annual N cycle is fed by storages of the soil in the model, indicating N depletion over time. Even though N losses of NO$_3^-$ and particularly N$_2$O emission (7 kg N ha^{-1} a^{-1}) have only a minor percentage in the total N balance, both rates are high regarding their environmental impact as a GHG contributing to global warming and as a water pollutant regarding eutrophication and drinking water supply, respectively. However, the uncertainty related to our estimated NO$_3^-$ leaching rate is overall the second largest uncertainty source in our N balance. These estimates cannot be sufficiently constraint with the given observation data, but they are in line with other reported N leaching rates on arable land in Germany (Siemens and Kaupenjohann, 2002).

The simulated N$_2$O emission contribute 3.1% to total simulated N losses. The underlying model runs follow the trend of the observation data. Hot moments can be observed after fertilizer applications, which are predicted by the model in time, but sometimes not in magnitude (e.g. March to May 2014). During these events, soil moisture is often not modeled accurately: The model predicts rewetting processes that have not been measured in the same magnitude (Fig. A1), which might explain the overestimated fluxes. A possible reason can also be uncertain rainfall model input data. Kavetski et al. (2006) found the measurements of precipitation within a catchment to be uncertain, as the trajectory of storm cells through a catchment may be different for each storm and may not have its center at the rain gauge where traditionally rainfall inputs are measured. Our rainfall data is measured 4 km northeast of the trace gas study area and is likely effected by such uncertainties.

For both, simulated and measured emissions on the arable site are highest in spring (Fig. 3). While the transects A1 and A2 vary with 95% of the values between 0 and 0.05 kg N_2O-N ha^{-1} day^{-1}, A3 shows a higher variation up to 0.15 kg N_2O-N ha^{-1} day^{-1}. As A3 is located at the hill toe, we attribute this effect to lateral transport of nitrate from uphill. However, our one-dimensional model set up does not cover lateral water and nutrition transport, accordingly the model is not

5 able to predict the higher emissions at A3 in spring. While such a process is part of complex integrated hydro-biogeochemical catchment models (Haas et al., 2013; Klatt et al., 2017; Wlotzka et al., 2013), it has not yet been confirmed experimentally. The distributions of the summer, autumn and winter seasons measured emissions are well in line with the modeled emissions. Furthermore, the modeled emissions are also in agreement with measured emissions before and after manure applications (Fig. 4). This result corresponds with a study of Molina-Herrera et al., (2016) who found LandscapeDNDC to be capable of

10 simulating agricultural N_2O emissions. However, in our case the model overestimates peak emissions before fertilizer applications, which leads to higher mean annual modeled emissions (7.33 kg N_2O-N ha^{-1} a^{-1}). This is 2.8 kg N_2O-N ha^{-1} a^{-1} higher than our observed emissions and even outside the large model uncertainty of 2.3 kg N_2O-N ha^{-1} a^{-1}. Hence, future research should particularly investigate the reason for this overestimation of peaks, either by revising the model structure or identification of other sources of model uncertainty.

15 Grassland N cycle: Grassland simulations consider an annual N input of 12.7 kg, with 7.6 kg coming from modeled biomass that is transferred into applied dung and urine through grazing sheep. Simulated N loss is substantially larger with 22.3 kg N ha^{-1} a^{-1} gaseous losses (primarily N_2), 1.5 kg N ha^{-1} a^{-1} occurring as nitrate leaching and 29.8 kg N ha^{-1} a^{-1} by biomass removal through grazing sheep and harvest (hay making). Comparing inputs and outputs, we simulated a mean nitrogen gap of 41 kg N ha^{-1} a^{-1}. Decreasing soil organic N stocks in model simulations indicate that the model is currently mimicking an additional

20 N source, which is not included in the current modelling approach. We assume uptake of additional N in form of nitrate by the shallow groundwater as a potential dominating process that is not included in the current LandscapeDNDC version we used. Liebermann et al. (2017) used a revised LandscapeDNDC set up for hypothesis testing to identify potential additional N sources in groundwater-dominated grasslands and showed, that groundwater N uptake is a likely contributor.

Taking a closer look at the modeled N_2O emissions, one can see that the model did not reproduce high as well as negative

25 (N_2O uptake) emissions. Currently, LandscapeDNDC does not consider any N_2O uptake, accordingly negative fluxes cannot be simulated by the model. The peaky dynamics of simulated N_2O emissions, especially from August 2014 to January 2015 are not confirmed by the measurements, indicating possible measurement errors in this time. One has also to consider the temporal mismatch of our weekly N_2O measurements and the hourly simulations, making a full match of observations versus simulations difficult.

30 There is no clear effect of grazing on the N_2O emissions on the grassland site in both measurements and modeled results (Fig. 4). Mean modeled annual emissions overestimate the observations by 0.4 kg N_2O-N ha^{-1} a^{-1}, and even the simulated uncertainty bounds of 0.27 kg N_2O-N ha^{-1} a^{-1} do not capture the measured dynamics.

Forest N cylce: N input is given for the forest model only by atmospheric deposition with an annual amount of 5.1 kg N ha^{-1} a^{-1}. Gaseous losses amount to 1.8 kg N ha^{-1} a^{-1}. Leaching contributes 0.6% of the N output. The rest (3.3 kg N ha^{-1} a^{-1}) is allocated

into biomass and soil. By taking a closer look on the N₂O emissions (Fig. 2), we see the model failing to reproduce the observed emission dynamics. Observed N₂O emissions have high error bars and not all transects are driven by frost-thaw cycles or N₂O uptake at the same time (Table 2). Parameterizing and simulating the forest transects independent from each other, would improve the simulations. One limiting factor is that both N₂O uptake and frost-thaw cycles are not included in the current

5   LandscapeDNDC version. We therefore recommend to particularly include frost-thaw cycles into the model (De Bruijn et al., 2009) as this process can have a major influence on N₂O inventories, e.g. up to 73% of the annual N₂O loss of a forest site in Högelwald, Germany (Papen and Butterbach-Bahl, 1999) was occurring during such cycles. The mean modeled annual emissions (0.33 kg N ha^{-1} a^{-1}) overestimate the observed emissions, but capture the mean observed annual emissions with their uncertainty bands of 0.15 kg N₂O-N ha^{-1} a^{-1}.
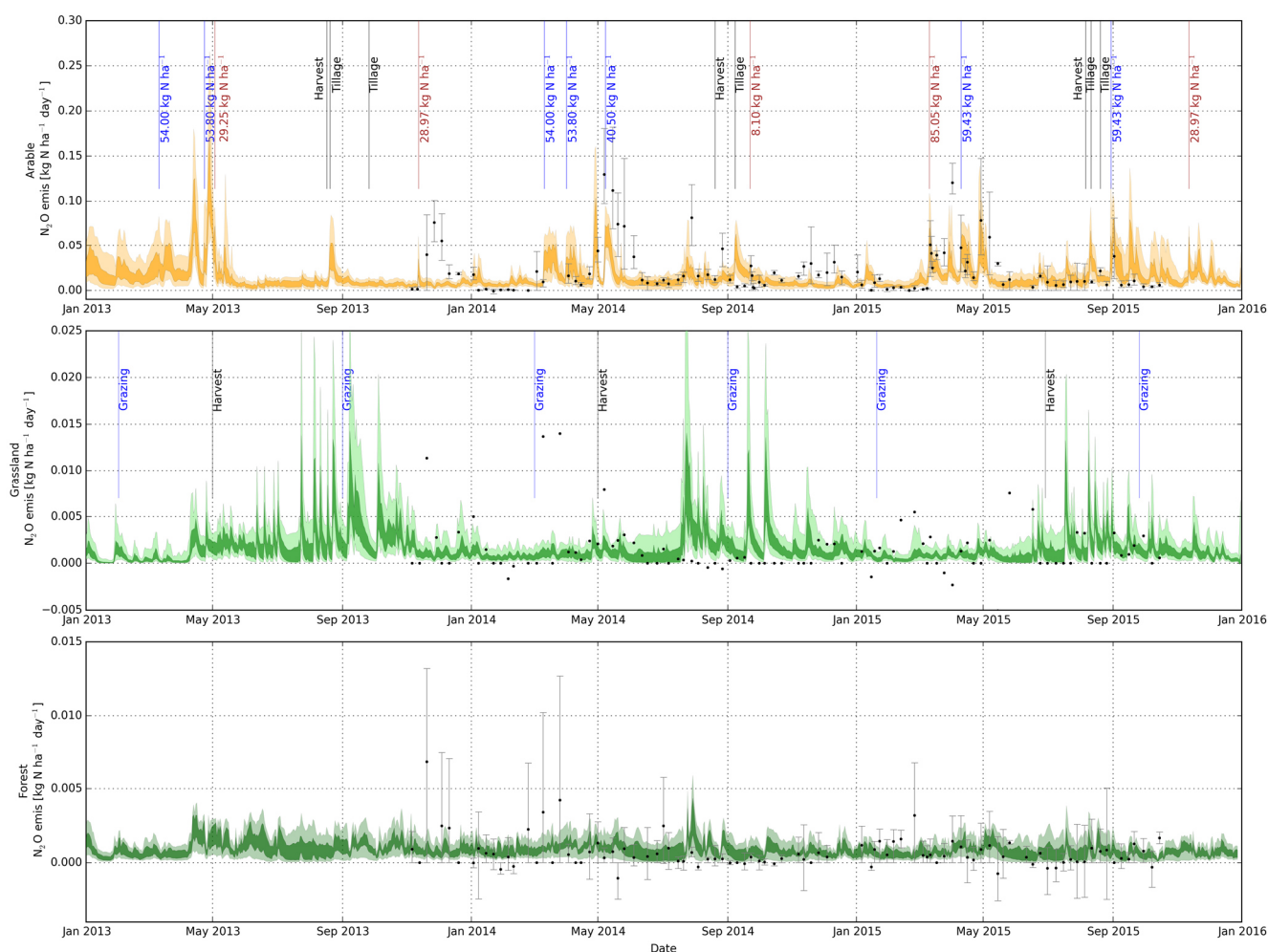
Figure 2: Measured and modeled N₂O emissions from different land use. Measurements are given as grey error bars showing the variance between the replicated transects and the mean value as a black dot. Posterior model uncertainty is given in light color for the 5 and 95 percentile and dark color for the 25 and 75 percentile. Vertical lines indicate management events. In the uppermost panel, blue colored vertical bars indicate fertilizer application, while brown color indicate manure application.
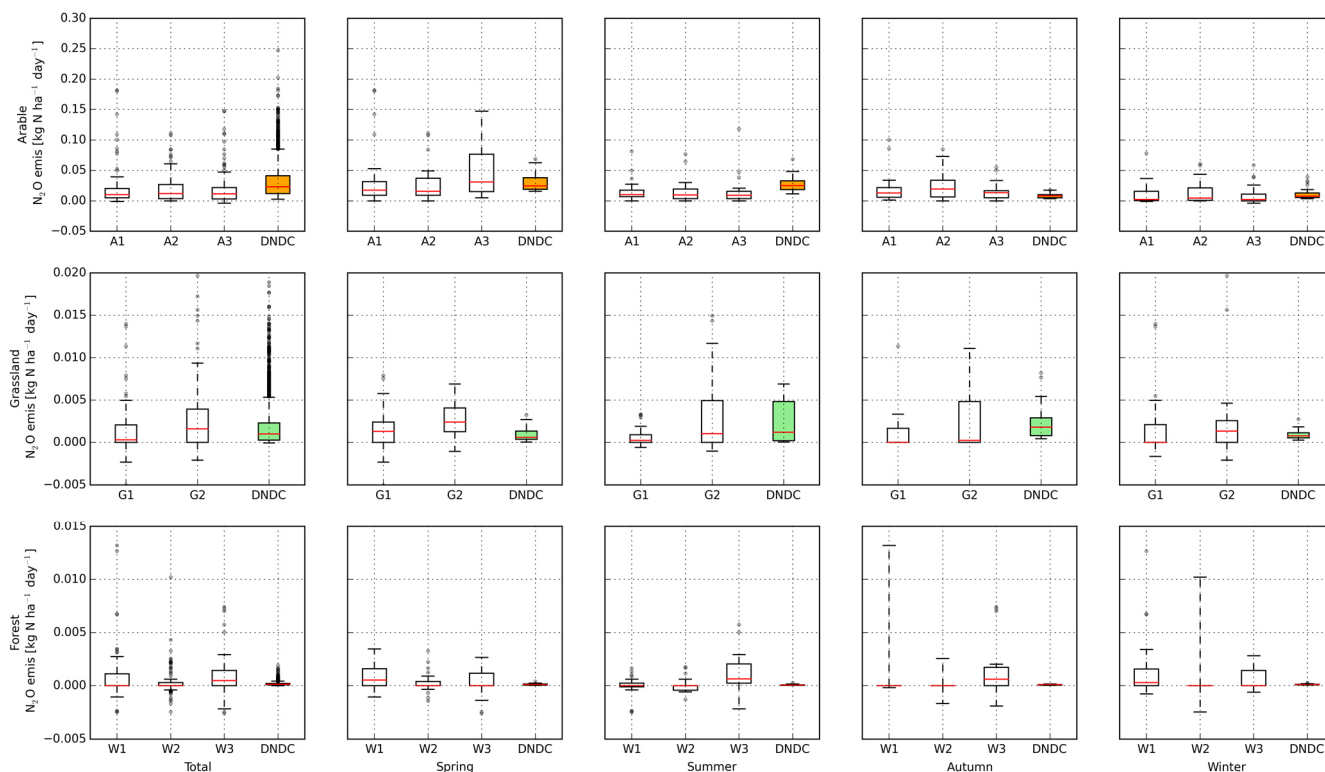
Figure 3: Observed and modeled N₂O emissions for spring (21.03 20.06.), summer (21.06. 20.09.), autumn (21.09. 20.12.), and winter (21.12. 20.03.).
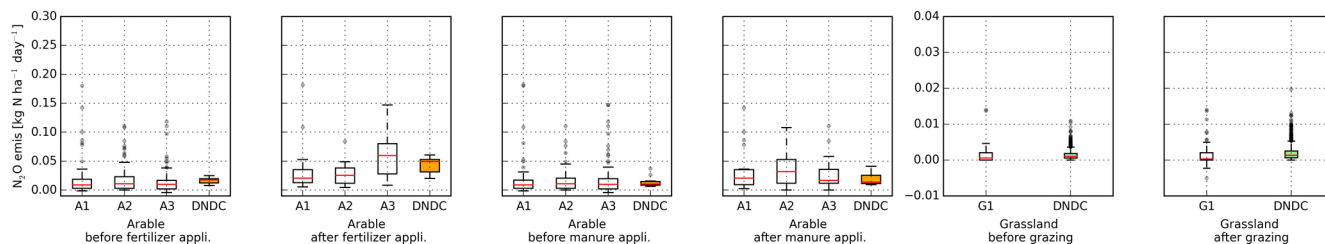
5   **Figure 4: Management effects on N₂O emissions. Measured and modeled emissions where selected in a time window of 2 weeks before and 2 weeks after a management.**

Table 4: Simulated nitrogen fluxes given by posterior model runs and their uncertainty on different land use in [kg N ha^{-1} a^{-1}]. N manure on grassland includes urine and dung input by sheep. Biomass output on grasslands combines harvest export and biomass leaving the system through sheep. Arable model assumes 20% return of stubble to field.

Modeled N flux	Arable		Grassland		Forest	
N deposition	5.11		5.11		5.11	
N manure	57.55		7.57		0	
N fertilizer	135.37		0		0	
Total input	**198.03**		**12.68**		**5.11**	
NO emis.	0.57	±0.16	0.46	±0.21	0.45	±0.33
N$_2$ emis.	62.55	±26.83	18.69	±10.91	1	±1.5
N$_2$O emis.	7.33	±2.3	0.69	±0.27	0.33	±0.15
NH$_3$ emis.	38.15	±20.8	2.45	±1.89	>0.01	±>0.01
Total gaseous output	**108.6**	**±50.09**	**22.29**	**±13.28**	**1.78**	**±1.98**
DON leaching	0.01	±>0.01	0.01	±>0.01	0.01	±>0.01
NO$_3$ leaching	30.01	±29.9	1.46	±3.19	0.03	±0.04
Total leaching output	**30.02**	**±29.9**	**1.47**	**±3.19**	**0.04**	**±0.04**
N grain export	63.92	±5.17	0		0	
N straw export	35.75	±2.67	29.77	±9.44	0	
Total biomass output	**99.67**	**±7.84**	**29.77**	**±9.44**	**0**	
Balance	**-40.26**	**±87.83**	**-40.85**	**±25.91**	**3.29**	**±2.02**

3.4 Modeled C fluxes

Modeled CO$_2$ emissions are shown for the different land uses over time (Fig. 5), separated into different seasons (Fig. 6) and before/after management-events occur (Fig. 7). The complete modeled C cycle is given in Table 5.

Arable C cycle: LandscapeDNDC simulations for the arable system predict a mean annual gross carbon uptake of 25.7 ± 1.3 t C-CO$_2$ ha^{-1} a^{-1}. 20.5 t C-CO$_2$ ha^{-1} a^{-1} leave the system through respiration, from which maintenance respiration contributes the largest proportion (65%). This is perfect in line with annual measured losses (Table 3). Harvest output is with 4.7 t C ha^{-1} a^{-1} in good agreement with the observed yields (Fig. A4). However, the temporal dynamic of the modeled TER on the arable study site underestimates the emissions in the summer season (Fig. 6) and mean modeled fluxes are substantially lower than measured ones (Fig. 7).

Tillage and harvest events fall into the summer season. While the observed emissions drop after harvest by 25%, the modeled emissions drop by even 50%. The reason for this is either an underestimation of the emissions through LandscapeDNDC (after harvest events until tillage occurs), or the uncertainty in the upscaling method of the measured CO$_2$ emissions (discussed in chapter 3.1.2). As microbial processes can oxidize more soil carbon after harvest (resulting in higher heterotrophic respiration),

we assume that the discrepancy is rather stemming from the model simulations. There are also studies, e.g. Buyanovsky et al. (1986), who report highest soil respiration rates after harvest. Modelled and measured soil CO_2 emissions agree well after tillage.

Grassland C cycle: LandscapeDNDC simulations for the grassland system predict a mean annual gross carbon uptake of 16.9 ± 1.7 t C-CO_2 ha^{-1} a^{-1} and an annual loss of 13.2 t C-CO_2 ha^{-1} a^{-1} through respiration. Further minor outputs are related to grazing (0.2 t C-CO_2 ha^{-1} a^{-1}), harvest (2.0 t C-CO_2 ha^{-1} a^{-1}) and allocation in the soil (1.4 t C-CO_2 ha^{-1} a^{-1}). Mean annual as well as temporal dynamics of modeled emissions are well in line with measured emissions. Effect of grazing has a minor influence on the total ecosystem respiration (Fig. 7), resulting in a wider range of both measured and modeled emissions. Grazing, i.e. reduction of root biomass, results in two contrary processes: reduction of maintenance respiration and increasing autotrophic respiration (Raich and Tufekciogul, 2000).

Forest C cycle: The forest model predicts an annual C input of 8.9 ± 0.6 t C-CO_2 ha^{-1} a^{-1} which is quite low compared to estimations for old-growth beech forests in Europe with reported rates from 14.4 to 18.3 t C-CO_2 ha^{-1} a^{-1} (Molina-Herrera et al., 2015). However, C uptake rates vary in magnitude with values presented from 3 to 34 t C-CO_2 ha^{-1} a^{-1} for different forests in different growing stages (Waring et al., 1998). As our study site is a mixture of young and old beech trees, we assume 40-50% less biomass compared to an old beech forest. Of the modeled C input, 6.6 t C-CO_2 ha^{-1} a^{-1} leave the system as gaseous CO_2. The rest is accumulated in the biomass and soil. Mean annual sum and dynamic of modeled emissions are in line with measured emissions. We expected to see rising emissions with litter fall in autumn (Raich and Tufekciogul, 2000), but cannot report this effect, neither with measurements, nor with model results (Fig. 6).
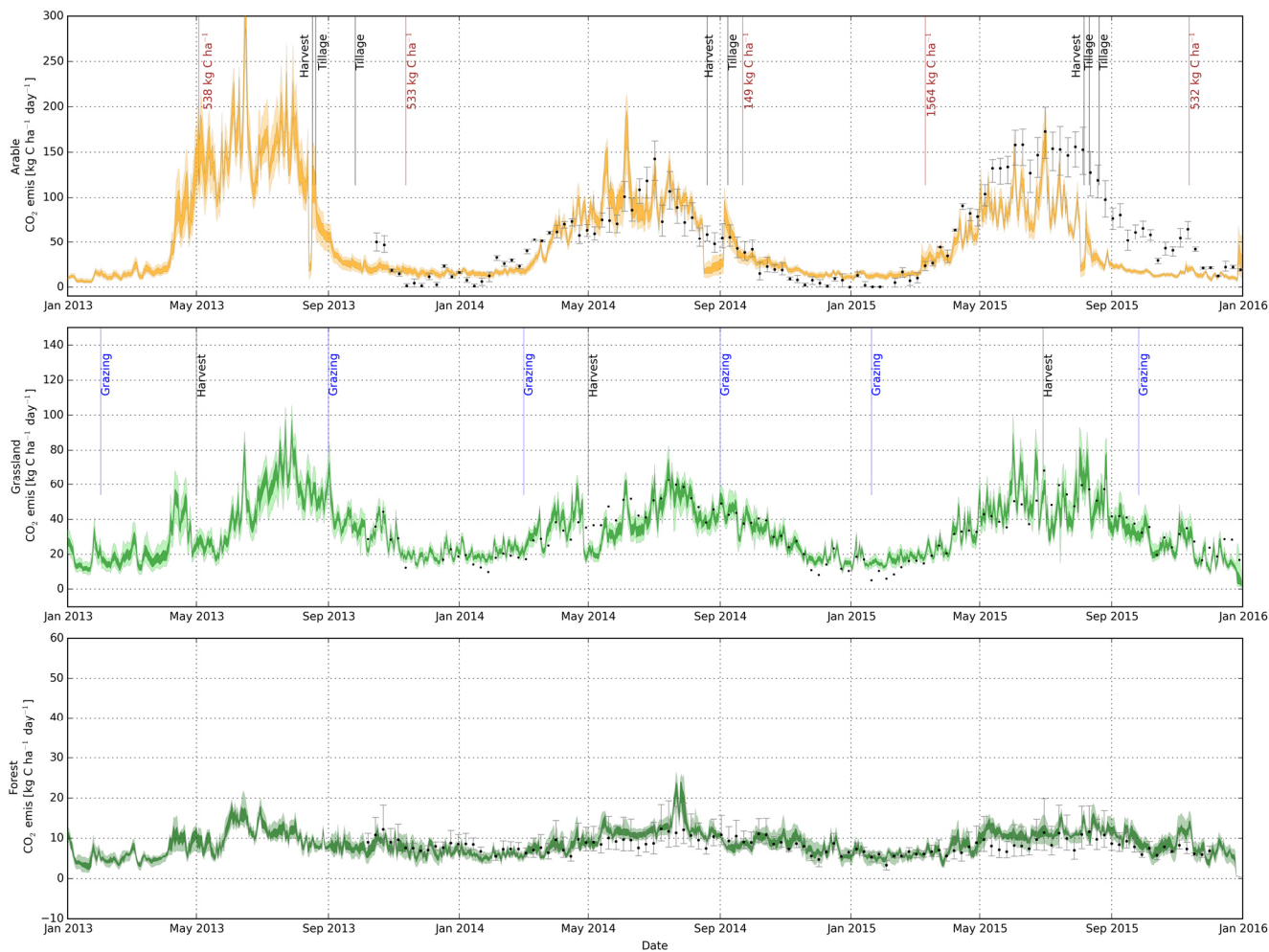
Figure 5: Modeled CO₂ emissions and management. Measurements are given as grey error bars showing the variance between the replicated transects and the mean value as a black dot. Posterior model uncertainty is given in light color for the 5 and 95 percentile and dark color for the 25 and 75 percentile. Vertical lines indicate management events. Brown colored bars in the uppermost panel indicate manure application.
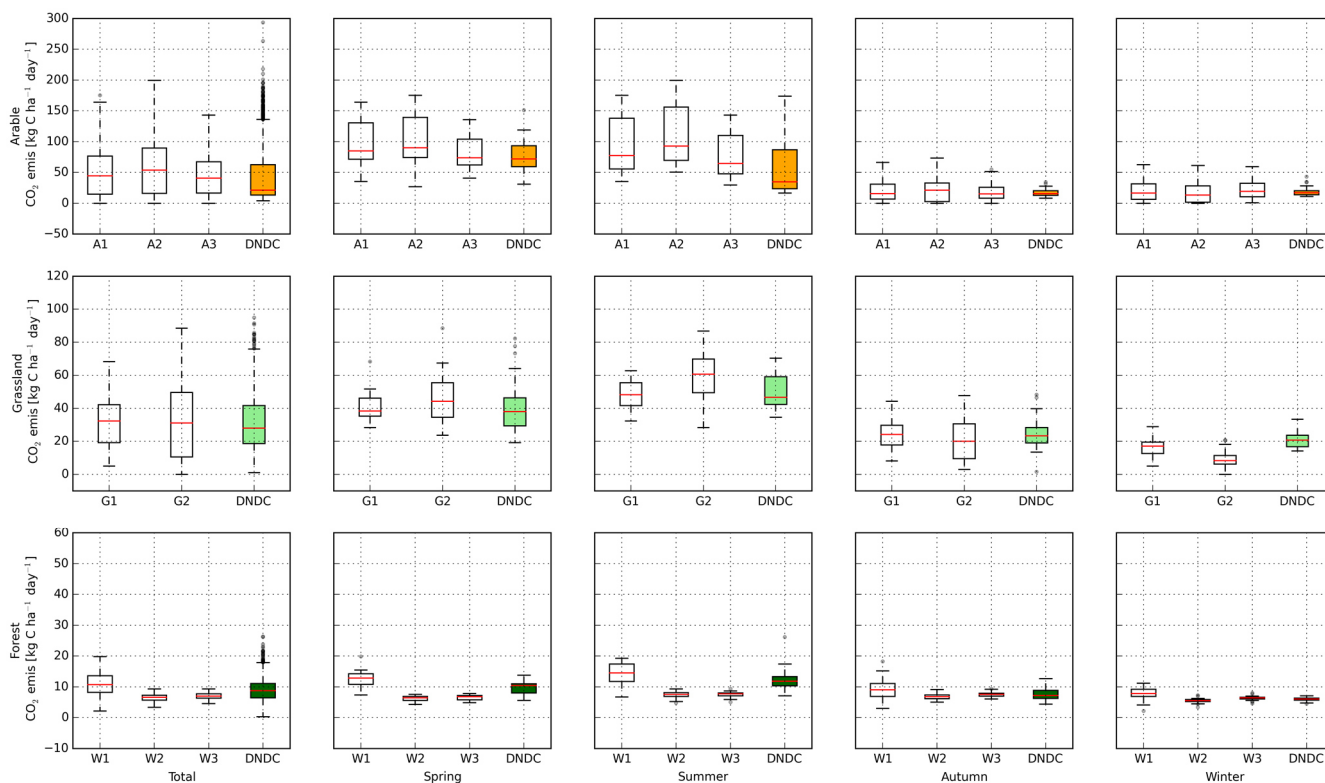
Figure 6: Observed and modeled CO₂ emissions for spring (21.03 20.06.), summer (21.06. 20.09.), autumn (21.09. 20.12.), and winter (21.12. 20.03.).
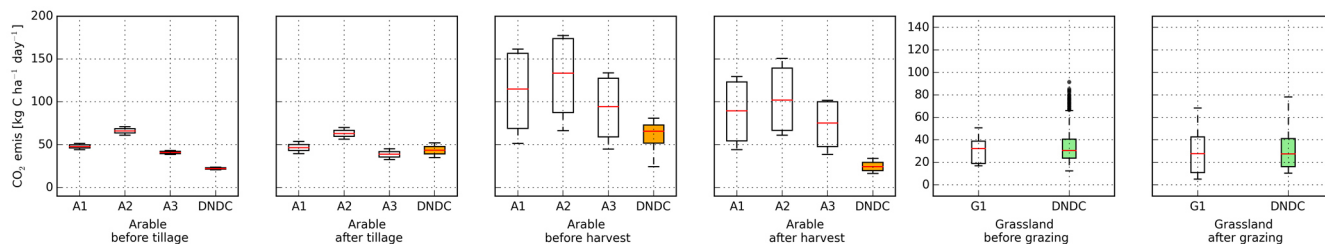
5   **Figure 7: Management effects on CO₂ emissions. Measured and modeled emissions where selected in a time window of 2 weeks before and 2 weeks after a management.**

Table 5: Simulated carbon fluxes given by posterior model runs and their uncertainty on different land use in [t C ha⁻¹ a⁻¹]. C manure on grassland includes input by sheep's dung. Arable model assumes 20% return of stubble to field.

Modeled C flux	Arable		Grassland		Forest	
CO$_2$ uptake	24.65	±1.32	16.8	±1.72	8.94	±0.56
C manure	1.06		0.07		0	
Total input	**25.71**	**±1.32**	**16.87**	**±1.72**	**8.94**	**±0.56**
Growth respiration	2.53	±0.2	0.81	±0.27	1.44	±0.05
Heterotrophic respiration	4.69	±0.53	2.27	±0.9	2.04	±0.1
Maintenance respiration	13.31	±1.06	10.16	±1.13	3.11	±0.39
Total gaseous output	**20.53**	**±1.79**	**13.24**	**±2.3**	**6.59**	**±0.54**
DOC leaching	>0.01	±>0.01	>0.01	±>0.01	>0.01	±>0.01
Total leaching output	**>0.01**		**>0.01**		**>0.01**	
C bud export	1.97	±0.17	0		0	
C straw export	2.75	±0.21	2.28	±0.72	0	
Total biomass output	**4.72**	**±0.38**	**2.28**	**±0.72**	**0**	
Balance	**0.46**	**±3.49**	**1.35**	**±4.74**	**2.35**	**±1.1**

4 Conclusion

We presented a two-year measurement campaign of trace gas emissions from adjacent land uses i.e. arable, grassland and

5   forest ecosystems with concurrent model development and rigorous testing through model-data fusion.

We found high emissions of N$_2$O and CO$_2$ on our arable sites, low emissions on grassland sites and lowest emissions on the forest sites. These observations enable us to investigate underlying effects of plant growth, temperature and WFPS, land use effects, seasonal patterns and management effects. Respiration amounts rise in less shaded (warmer) areas of the forest, while N$_2$O emissions increase toward the foot of the hills of forest and arable sites due to nitrogen accumulation. Highly variable

10   N$_2$O emissions in forest resulted in large uncertainty of model verification data and was translated in large uncertainty of model results for forest.

Detailed measured data of soil and management allowed fitting the biogeochemical model LandscapeDNDC to the measured soil moisture, yield and GHG emissions of CO$_2$ and N$_2$O. Overall, model performance is classified in Table 6.

The model reproduced measured data reasonably well in time, separated into seasons and management events. Model

15   performance was best in predicting management effects on N$_2$O emissions and annual CO$_2$ emissions for all land uses. With regard to land use, simulations for grassland sites work best, followed by those for arable land. Simulations for N$_2$O emissions on arable land outperform those for CO$_2$, and vice versa for grassland. Low emissions on forest sites were generally difficult to depict by our modeling approach.

The model-data fusion approach allowed us to derive model structural deficiencies that would likely increase model performances if implemented in Landscape DNDC: (1) missing N_2O uptake processes; (2) missing NO_3^- (and potentially dissolved organic nitrogen) uptake through shallow groundwater; (3) missing lateral interaction at hillslopes due to 1D model set up.

5 **Table 6: Overall posterior model performance of LandscapeDNDC on different land use in reproducing GHG emission data. Classified into (1) good, (2) medium and (3) poor model performance in simulating reliable annual sums, seasonal patterns and magnitude of management events (e.g. fertilizer application). NA = not applicable, i.e. no forest management during modeled period from 2010-2016.**

Modelled performance on each land use	N_2O emissions			CO_2 emissions		
	annual	seasonal	management	annual	seasonal	management
Arable (A1-3)	2	1	1	1	2	3
Grassland (G1)	1	2	1	1	1	1
Forest (W1-W3)	2	2	NA	1	2	NA

10 Furthermore, posterior model runs allowed quantifying magnitude and uncertainty of not measured fluxes of the C and N cycle. Investigated forest site is in general acting as the largest sink for C and N, with annual sequestration rates of 2.4 t C ha^{-1} and 3.3 kg N ha^{-1}. The extensive grazed grassland is also acting as a sink for C with 1.4 t C ha^{-1} per year, while the N cycle of the grassland model cannot be closed with the given settings. Shrinking N soil pools indicate a missing input, which we assume from shallow groundwater with additional N supply of around 40 kg N ha^{-1} a^{-1}.

15 Current land use in this catchment is dominated by forests (37%) and arable land (35%), whereas grassland sites (11%) are mainly distributed along the stream. Under the viewpoint of climate smart landscapes, measured data suggests the benefit of forests in a landscape, having the least GHG emissions. Riparian zones can act as sinks of N, but only during the vegetation period and times when roots have access to groundwater. Arable land use produces high amounts of N_2O, but not throughout the year, rather in spring after fertilizer application.

20 Potential interactions of land use pattern cannot be quantified with the current one dimensional model approach. However, the dataset could be used in future studies to quantify nitrate uptake of riparian zones in more detail, e.g. by coupling LandscapeDNDC to a hydrological model as done by Klatt et al. (2017). Such a model setup would also allow an upscaling in space, e.g. for generation of GHG inventories or an analysis of more detailed management scenarios in time.

Code availability

25 The LandscapeDNDC framework is free available upon request from www.svn.imk-ifu.kit.edu

The SPOTPY tool, used for model-data fusion, is free open source and available from www.pypi.python.org/pypi/spotpy

Data availability

All measured data is free available upon request from www.fb09-pasig.umwelt.uni-giessen.de:8081

Appendices
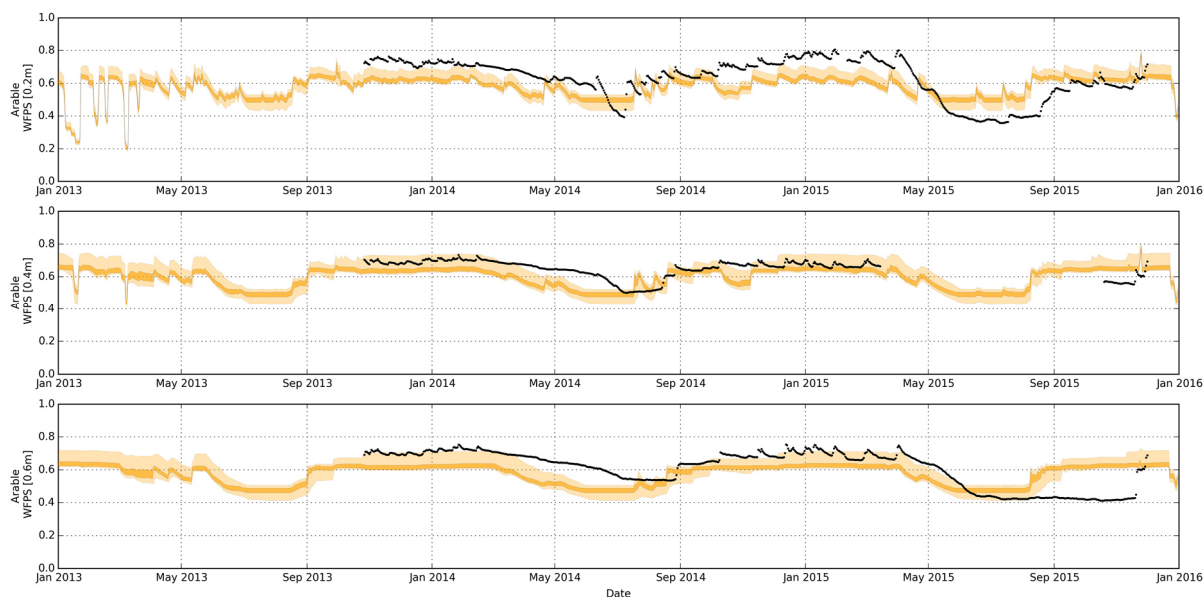
5   **Figure A1: Modeled WFPS on arable land in different depths. RMSEs ranging from 0.0774 to 0.1194% WFPS [0.2m], 0.0511 to 0.0955% WFPS [0.4m] and 0.0921 to 0.1193% WFPS [0.6m].**
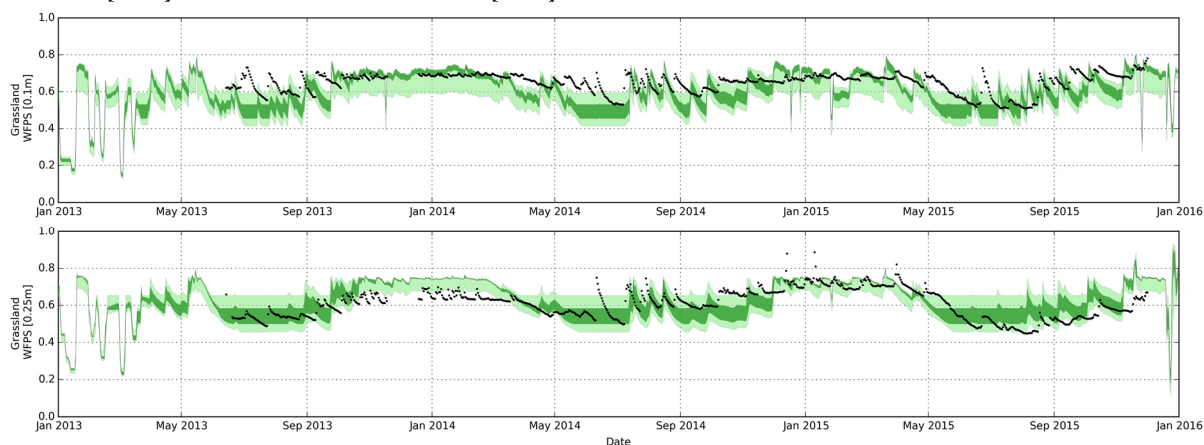
Figure A2: Modeled WFPS on grassland in different depths. RMSEs ranging from 0.043 to 0.1481% WFPS [0.1m] and 0.056 0.1069% WFPS [0.25m].
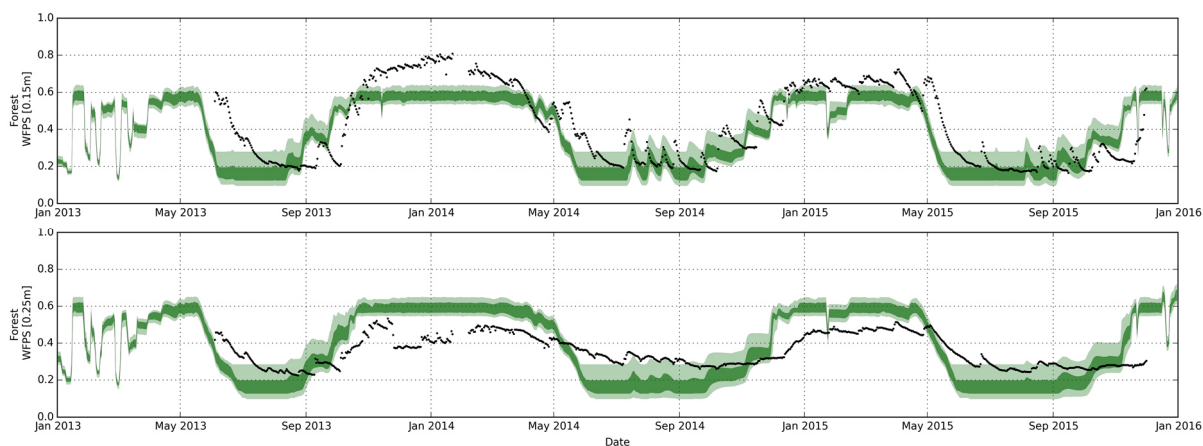
Figure A3: Modeled WFPS on forest in different depths. RMSEs ranging from 0.0817 to 0.1324% WFPS [0.15m] and 0.0812 to 0.1606% WFPS [0.25m].
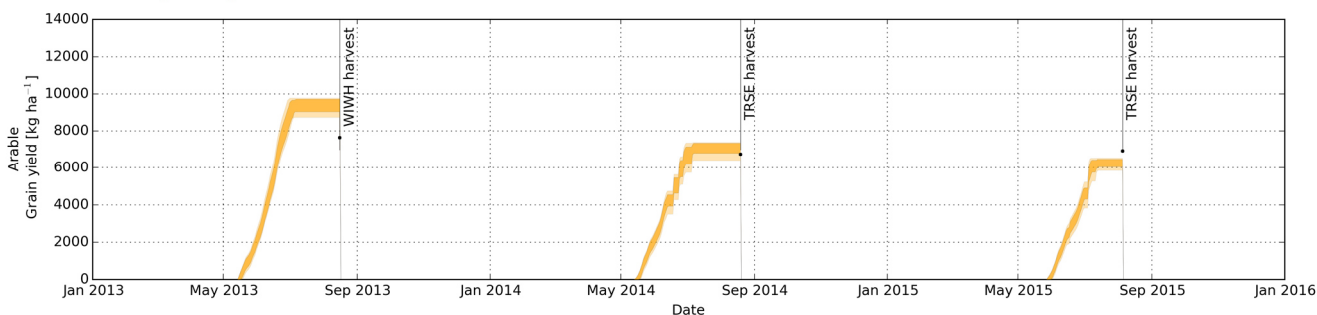
5 **Figure A4: Modeled dry weight grain yield on arable land use. WIWH = Winter wheat, TRSE = Triticum secale. RMSEs ranging from 1125.7 to 2529.2 kg ha^{-1}.**
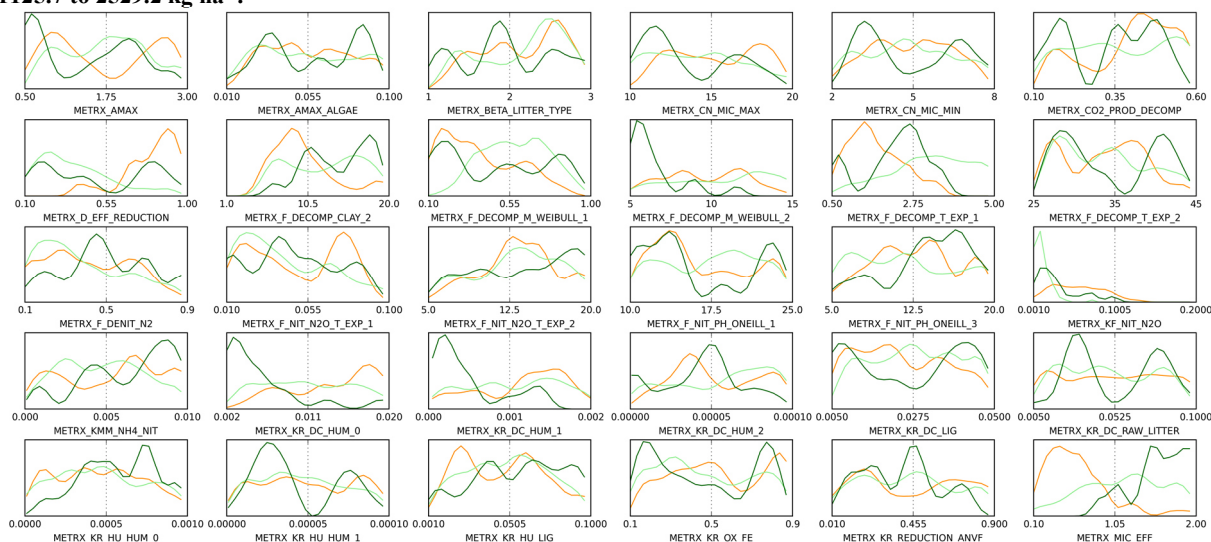
Figure A5: Posterior parameter distribution of the LandscapeDNDC module MeTrx. Orange line = arable, light green line = grassland, dark green line = forest model set up.
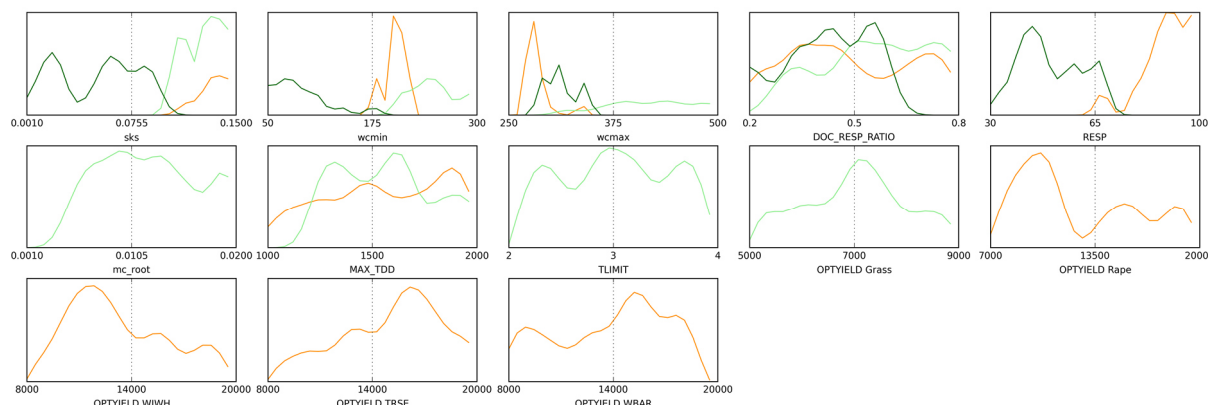
Figure A6: Posterior parameter distribution of the LandscapeDNDC modules wcDNDC and physiology. Orange line = arable, light green line = grassland, dark green line = forest model set up.

Table A1: Input parameters for all investigated LandscapeDNDC modules with uniform distribution for Latin Hypercube Sampling. FASY = Fagus sylvatica, PERG = Perennial grass.

module	parameter name	Description	min	max
wcDNDC	sks_arable	Value of soil layer for saturated hydraulic conductivity	0.1	0.2
wcDNDC	sks_grassland	Value of soil layer for saturated hydraulic conductivity	0.1	0.15
wcDNDC	sks_forest	Value of soil layer for saturated hydraulic conductivity	0.1	0.1
wcDNDC	wcmin_arable	Wilting point of soil layer	170	220
wcDNDC	wcmin_grassland	Wilting point of soil layer	200	300
wcDNDC	wcmin_forest	Wilting point of soil layer	40	200
wcDNDC	wcmax_arable	Field capacity of uppermost soil layer	270	350
wcDNDC	wcmax_grassland	Field capacity of soil layer	300	500
wcDNDC	wcmax_forest	Field capacity of soil layer	270	350
physiology	DOC_RESP_RATIO_FASY	Ratio of root exudates related to root growth respiration	0.1	0.6
physiology	RESP_FASY	Factor determining plant respiration	30	70
physiology	DOC_RESP_RATIO_PERG	Ratio of root exudates related to root growth respiration	0.2	0.8
physiology	MC_ROOT_PERG	Maintenance respiration coefficient of roots	0.001	0.02
physiology	MAX_TDD_PERG	Temperature degree days for full plant development	1200	2000
physiology	OPTYIELD_PERG	Optimum yield of crops and grasses	5000	9000
physiology	TLIMIT_PERG	Temperature limit for plant growth	2	4
physiology	DOC_RESP_RATIO_arable	Ratio of root exudates related to root growth respiration	0.2	0.8
physiology	MAX_TDD_arable	Temperature degree days for full plant development	1000	2000
physiology	RESP_arable	Factor determining plant respiration	30	100
physiology	OPTYIELD_rape	Optimum yield of Rape	7000	20000
physiology	OPTYIELD_WIWH	Optimum yield of Winter Wheat	8000	20000
physiology	OPTYIELD_TRSE	Optimum yield of Triticale	8000	20000
physiology	OPTYIELD_WBAR	Optimum yield of Winter Barley	8000	20000
METRX	METRX_AMAX	Maximum microbial death rate	0.5	3
METRX	METRX_AMAX_ALGAE	Maximum decay rate of alga	0.01	0.1
METRX	METRX_BETA_LITTER_TYPE	Exp. fac. of litter decomposition red. depend. on lignin conc	1	3
METRX	METRX_CN_MIC_MAX	Maximum allowed C:N ratio for microbes	10	20

METRX	METRX_CN_MIC_MIN	Minimum allowed C:N ratio for microbes	2	8
METRX	METRX_CO2_PROD_DECOMP	Instantaneously production of CO_2 during decomposition	0.1	0.6
METRX	METRX_D_EFF_REDUCTION	Reduction factor for gas diffusion	0.1	1
METRX	METRX_F_DECOMP_CLAY_2	Factor for clay dependency of decomposition	1	20
METRX	METRX_F_DECOMP_M_WEIBULL_1	Factor for water filled pore space dependency of decomposition	0.1	1
METRX	METRX_F_DECOMP_M_WEIBULL_2	Factor for water filled pore space dependency of decomposition	5	15
METRX	METRX_F_DECOMP_T_EXP_1	Factor for temperature dependency of decomposition	0.5	5
METRX	METRX_F_DECOMP_T_EXP_2	Factor for temperature dependency of decomposition	25	45
METRX	METRX_F_DENIT_N2	Factor determining amount denitrified nitrogen goes to N2	0.1	0.9
METRX	METRX_F_NIT_N2O_T_EXP_1	Factor for temp. depend. of N2O prod. during nitrification	0.01	0.1
METRX	METRX_F_NIT_N2O_T_EXP_2	Factor for temperature dependency of N2O production	5	20
METRX	METRX_F_NIT_PH_ONEILL_1	Factor for pH dependency of nitrification	10	25
METRX	METRX_F_NIT_PH_ONEILL_3	Factor for pH dependency of nitrification	5	20
METRX	METRX_KF_NIT_N2O	Maximum fraction of nitrified NH4 that goes to N2O	0.001	0.2
METRX	METRX_KMM_NH4_NIT	Michaelis-Menten const. for NH4 depend. of nitrification	0.00001	0.01
METRX	METRX_KR_DC_HUM_0	Decomposition constant of recalcitrant young humus	0.002	0.02
METRX	METRX_KR_DC_HUM_1	Decomposition constant of recalcitrant old humus	0.00005	0.002
METRX	METRX_KR_DC_HUM_2	Decomposition constant of recalcitrant old humus	0.000001	0.0001
METRX	METRX_KR_DC_LIG	Decomposition constant of lignin	0.0005	0.05
METRX	METRX_KR_DC_RAW_LITTER	Decomposition constant of raw litter	0.005	0.1
METRX	METRX_KR_HU_HUM_0	Rate constant for humification of labile humus to recalcitrant young humus	0.000001	0.001
METRX	METRX_KR_HU_HUM_1	Rate constant for humification of recalcitrant young humus to recalcitrant old humus	0.000001	0.0001
METRX	METRX_KR_HU_LIG	Rate constant for humification of lignin	0.0001	0.1
METRX	METRX_KR_OX_FE	Rate constant of iron oxidation	0.1	0.9
METRX	METRX_KR_REDUCTION_ANVF	Decomposition reduction due anaerobicity	0.01	0.9
METRX	METRX_MIC_EFF	Microbial carbon use efficiency	0.1	2

Author contribution

T. Houska, L. Breuer and R. Kiese designed and managed the experiments. D. Kraus and T. Houska performed the simulations.

T. Houska prepared the manuscript with contributions from all co-authors.

Competing interests

5 The authors declare that they have no conflict of interest.

Acknowledgements

We acknowledge the financial support provided by the Deutsche Forschungsgemeinschaft (DFG) for Tobias Houska (BR2238/13-1). Special thanks deserves Felix Kruck, Eva Holthof and Michael Herzog for their fieldwork during any weather conditions, Anja Schaefler-Schmid and Julia Valverde for lab analysis and providing the chamber sampling equipment as well
5   as the farmer, for letting us study his land and providing the detailed management information.

References

Arias-Navarro, C., Díaz-Pinés, E., Kiese, R., Rosenstock, T. S., Rufino, M. C., Stern, D., Neufeldt, H., Verchot, L. V. and Butterbach-Bahl, K.: Gas pooling: A sampling technique to overcome spatial heterogeneity of soil carbon dioxide and nitrous oxide fluxes, Soil Biol. Biochem., 67, 20–23, doi:10.1016/j.soilbio.2013.08.011, 2013.

10   Barton, L., Kiese, R., Gatter, D., Butterbach-Bahl, K., Buck, R., Hinz, C. and Murphy, D. V.: Nitrous oxide emissions from a cropped soil in a semi-arid climate, Glob. Change Biol., 14(1), 177–192, 2008.

Beven, K. and Binley, A.: The future of distributed models: Model calibration and uncertainty prediction, Hydrol. Process., 6(3), 279–298, doi:10.1002/hyp.3360060305, 1992.

Bloom, A. A. and Williams, M.: Constraining ecosystem carbon dynamics in a data-limited world: integrating ecological
15   "common sense" in a model-data fusion framework, Biogeosciences, 12(5), 1299, 2015.

Boden, T. A., Marland, G. and Andres, R. J.: Global, regional and national fossil fuel co2 emissions. [online] Available from: http://cdiac.ornl.gov/trends/emis/overview_2007.html (Accessed 17 August 2016), 2010.

Bouwman, A. F., Boumans, L. J. M. and Batjes, N. H.: Emissions of N2O and NO from fertilized fields: Summary of available measurement data, Glob. Biogeochem. Cycles, 16(4), 2002.

20   Bremner, J. M.: Sources of nitrous oxide in soils, Nutr. Cycl. Agroecosystems, 49(1–3), 7–16, 1997.

Burton, D. L., Li, X. and Grant, C. A.: Influence of fertilizer nitrogen source and management practice on N2O emissions from two Black Chernozemic soils, Can. J. Soil Sci., 88(2), 219–227, 2008.

Butterbach-Bahl, K., Baggs, E. M., Dannenmann, M., Kiese, R. and Zechmeister-Boltenstern, S.: Nitrous oxide emissions from soils: how well do we understand the processes and their controls?, Philos. Trans. R. Soc. Lond. B Biol. Sci., 368(1621),
25   20130122, doi:10.1098/rstb.2013.0122, 2013.

Buyanovsky, G. A., Wagner, G. H. and Gantzer, C. J.: Soil respiration in a winter wheat ecosystem, Soil Sci Soc Am J, 50(2), 338–344, 1986.

Cole, C. V., Duxbury, J., Freney, J., Heinemeyer, O., Minami, K., Mosier, A., Paustian, K., Rosenberg, N., Sampson, N. and Sauerbeck, D.: Global estimates of potential mitigation of greenhouse gas emissions by agriculture, Nutr. Cycl.
30   Agroecosystems, 49(1–3), 221–228, 1997.

De Bruijn, A. M. G., Butterbach-Bahl, K., Blagodatsky, S. and Grote, R.: Model evaluation of different mechanisms driving freeze–thaw N2O emissions, Agric. Ecosyst. Environ., 133(3), 196–207, 2009.

Flechard, C. R., Neftel, A., Jocher, M., Ammann, C. and Fuhrer, J.: Bi-directional soil/atmosphere N2O exchange over two mown grassland systems with contrasting management practices, Glob. Change Biol., 11(12), 2114–2127, 2005.

Flechard, C. R., Nemitz, E., Smith, R. I., Fowler, D., Vermeulen, A. T., Bleeker, A., Erisman, J. W., Simpson, D., Zhang, L. and Tang, Y. S.: Dry deposition of reactive nitrogen to European ecosystems: a comparison of inferential models across the NitroEurope network, Atmospheric Chem. Phys., 11(6), 2703–2728, 2011.

Gabrielle, B., Laville, P., Duval, O., Nicoullaud, B., Germon, J.-C. and Hénault, C.: Process-based modeling of nitrous oxide emissions from wheat-cropped soils at the subregional scale, Glob. Biogeochem. Cycles, 20(4), 2006.

Gilmanov, T. G., Soussana, J. F., Aires, L., Allard, V., Ammann, C., Balzarolo, M., Barcza, Z., Bernhofer, C., Campbell, C. L. and Cernusca, A.: Partitioning European grassland net ecosystem CO 2 exchange into gross primary productivity and ecosystem respiration using light response function analysis, Agric. Ecosyst. Environ., 121(1), 93–120, 2007.

Giltrap, D. L., Li, C. and Saggar, S.: DNDC: A process-based model of greenhouse gas fluxes from agricultural soils, Agric. Ecosyst. Environ., 136(3–4), 292–300, doi:10.1016/j.agee.2009.06.014, 2010.

Glatzel, S. and Stahr, K.: Methane and nitrous oxide exchange in differently fertilised grassland in southern Germany, Plant Soil, 231(1), 21–35, 2001.

Graedel, T. E. and Crutzen, P. J.: The changing atmosphere., Sci. Am., 58–68, 1989.

Haas, E., Klatt, S., Fröhlich, A., Kraft, P., Werner, C., Kiese, R., Grote, R., Breuer, L. and Butterbach-Bahl, K.: LandscapeDNDC: a process model for simulation of biosphere–atmosphere–hydrosphere exchange processes at site and regional scale, Landsc. Ecol., 28(4), 615–636, doi:10.1007/s10980-012-9772-x, 2013.

Houska, T., Kraft, P., Chamorro-Chavez, A. and Breuer, L.: SPOTting Model Parameters Using a Ready-Made Python Package, PLoS ONE, 10(12), e0145180, doi:10.1371/journal.pone.0145180, 2015.

Houska, T., Kraft, P., Liebermann, R., Klatt, S., Kraus, D., Haas, E., Santabárbara, I., Kiese, R., Butterbach-Bahl, K., Müller, C. and Breuer, L.: Rejecting hydro-biogeochemical model structures by multi-criteria evaluation, Environ. Model. Softw., 93, 1–12, doi:10.1016/j.envsoft.2017.03.005, 2017.

IPCC: Revised 1996 IPCC guidelines for national greenhouse gas inventories. v. 1: Greenhouse gas inventory reporting instructions.-v. 2: Greenhouse gas inventory workbook.-v. 3: Greenhouse gas inventory reference manual, 1997.

IPCC: Contribution of working group III to the fourth assessment report of the intergovernmental panel on climate change, 2007.

Janssens, I. A., Lankreijer, H., Matteucci, G., Kowalski, A. S., Buchmann, N., Epron, D., Pilegaard, K., Kutsch, W., Longdoz, B. and Grünwald, T.: Productivity overshadows temperature in determining soil and ecosystem respiration across European forests, Glob. Change Biol., 7(3), 269–278, 2001.

Jansson, P.-E.: CoupModel: model use, calibration, and validation, Trans. ASABE, 55(4), 1337–1344, 2012.

Jungkunst, H. F., Freibauer, A., Neufeldt, H. and Bareth, G.: Nitrous oxide emissions from agricultural land use in Germany— a synthesis of available annual field data, J. Plant Nutr. Soil Sci., 169(3), 341–351, 2006.

Kammann, C., Grünhage, L., Müller, C., Jacobi, S. and Jäger, H.-J.: Seasonal variability and mitigation options for N2O emissions from differently managed grasslands, Environ. Pollut., 102, 179–186, doi:10.1016/S0269-7491(98)80031-6, 1998.

Kavetski, D., Kuczera, G. and Franks, S. W.: Bayesian analysis of input uncertainty in hydrological modeling: 1. Theory, Water Resour. Res., 42(3), W03407, doi:10.1029/2005WR004368, 2006.

Keenan, T. F., Carbone, M. S., Reichstein, M. and Richardson, A. D.: The model–data fusion pitfall: assuming certainty in an uncertain world, Oecologia, 167(3), 587, 2011.

5 Kiese, R., Heinzeller, C., Werner, C., Wochele, S., Grote, R. and Butterbach-Bahl, K.: Quantification of nitrate leaching from German forest ecosystems by use of a process oriented biogeochemical model, Environ. Pollut., 159(11), 3204–3214, doi:10.1016/j.envpol.2011.05.004, 2011.

Kim, Y., Seo, Y., Kraus, D., Klatt, S., Haas, E., Tenhunen, J. and Kiese, R.: Estimation and mitigation of N2O emission and nitrate leaching from intensive crop cultivation in the Haean catchment, South Korea, Sci. Total Environ., 529, 40–53, 10 doi:10.1016/j.scitotenv.2015.04.098, 2015.

Klatt, S., Kraus, D., Kraft, P., Breuer, L., Wlotzka, M., Heuveline, V., Haas, E., Kiese, R. and Butterbach-Bahl, K.: Exploring impacts of vegetated buffer strips on nitrogen cycling using a spatially explicit hydro-biogeochemical modeling approach, Environ. Model. Softw., 90, 55–67, 2017.

Kraus, D., Weller, S., Klatt, S., Haas, E., Wassmann, R., Kiese, R. and Butterbach-Bahl, K.: A new LandscapeDNDC 15 biogeochemical module to predict CH4 and N2O emissions from lowland rice and upland cropping systems, Plant Soil, 386(1–2), 125–149, doi:10.1007/s11104-014-2255-x, 2015.

Liebermann, R., Houska, T., Kraft, P., Klatt, S., Kraus, D., Haas, E., Müller, C. and Breuer, L.: Closing the N-budget: How Simulated Groundwater-borne Nitrate Supply Affects Plant Growth and Greenhouse Gas Emissions on a Temperate Grassland, PLoS ONE, submitted, 2017.

20 Lohila, A., Aurela, M., Regina, K. and Laurila, T.: Soil and total ecosystem respiration in agricultural fields: effect of soil and crop type, Plant Soil, 251(2), 303–317, 2003.

Molina-Herrera, S., Grote, R., Santabárbara-Ruiz, I., Kraus, D., Klatt, S., Haas, E., Kiese, R. and Butterbach-Bahl, K.: Simulation of CO2 Fluxes in European Forest Ecosystems with the Coupled Soil-Vegetation Process Model "LandscapeDNDC," Forests, 6(6), 1779–1809, doi:10.3390/f6061779, 2015.

25 Molina-Herrera, S., Haas, E., Klatt, S., Kraus, D., Augustin, J., Magliulo, V., Tallec, T., Ceschia, E., Ammann, C. and Loubet, B.: A modeling study on mitigation of N 2 O emissions and NO 3 leaching at different agricultural sites across Europe using LandscapeDNDC, Sci. Total Environ., 553, 128–140, doi:10.1016/j.scitotenv.2015.12.099, 2016.

Myhre, G., Shindell, D., Bréon, F.-M., Collins, W., Fuglestvedt, J., Huang, J., Koch, D., Lamarque, J.-F., Lee, D. and Mendoza, B.: Anthropogenic and natural radiative forcing, Clim. Change, 423, 2013.

30 Neftel, A., Flechard, C., Ammann, C., Conen, F., Emmenegger, L. and Zeyer, K.: Experimental assessment of N2O background fluxes in grassland systems, Tellus B, 59(3), 470–482, 2007.

Oenema, O., Velthof, G. L., Yamulki, S. and Jarvis, S. C.: Nitrous oxide emissions from grazed grassland, Soil Use Manag., 13(s4), 288–295, 1997.

Orlowski, N., Kraft, P., Pferdmenges, J. and Breuer, L.: Exploring water cycle dynamics by sampling multiple stable water 35 isotope pools in a developed landscape in Germany, Hydrol. Earth Syst. Sci., 20(9), 3873, 2016.

Papen, H. and Butterbach-Bahl, K.: A 3-year continuous record of nitrogen trace gas fluxes from untreated and limed soil of a N-saturated spruce and beech forest ecosystem in Germany: 1. N2O emissions, J. Geophys. Res. Atmospheres, 104(D15), 18487–18503, 1999.

Parsons, A. J.: The effects of season and management on the growth of grass swards, in The grass crop, pp. 129–177, Springer., 1988.

Parton, W. J., Hartman, M., Ojima, D. and Schimel, D.: DAYCENT and its land surface submodel: description and testing, Glob. Planet. Change, 19(1–4), 35–48, doi:10.1016/S0921-8181(98)00040-X, 1998.

Raich, J. W. and Schlesinger, W. H.: The global carbon dioxide flux in soil respiration and its relationship to vegetation and climate, Tellus B, 44(2), 81–99, 1992.

Raich, J. W. and Tufekciogul, A.: Vegetation and soil respiration: correlations and controls, Biogeochemistry, 48(1), 71–90, 2000.

Ravishankara, A. R., Daniel, J. S. and Portmann, R. W.: Nitrous oxide (N2O): the dominant ozone-depleting substance emitted in the 21st century, science, 326(5949), 123–125, 2009.

Rochette, P., Flanagan, L. B. and Gregorich, E. G.: Separating soil respiration into plant and soil components using analyses of the natural abundance of carbon-13, Soil Sci. Soc. Am. J., 63(5), 1207–1213, 1999.

Savage, K., Phillips, R. and Davidson, E.: High temporal frequency measurements of greenhouse gas emissions from soils, Biogeosciences, 11(10), 2709–2720, 2014.

Seifert, A.-G., Roth, V.-N., Dittmar, T., Gleixner, G., Breuer, L., Houska, T. and Marxsen, J.: Comparing molecular composition of dissolved organic matter in soil and stream water: Influence of land use and chemical characteristics, Sci. Total Environ., 571, 142–152, 2016.

Siemens, J. and Kaupenjohann, M.: Contribution of dissolved organic nitrogen to N leaching from four German agricultural soils, J. Plant Nutr. Soil Sci., 165(6), 675–681, 2002.

Smith, K. A., Ball, T., Conen, F., Dobbie, K. E., Massheder, J. and Rey, A.: Exchange of greenhouse gases between soil and atmosphere: interactions of soil physical factors and biological processes, Eur. J. Soil Sci., 54(4), 779–791, 2003.

Soussana, J. F., Allard, V., Pilegaard, K., Ambus, P., Amman, C., Campbell, C., Ceschia, E., Clifton-Brown, J., Czóbel, S. Z. and Domingues, R.: Full accounting of the greenhouse gas (CO2, N2O, CH4) budget of nine European grassland sites, Agric. Ecosyst. Environ., 121(1), 121–134, 2007.

Subke, J.-A., Reichstein, M. and Tenhunen, J. D.: Explaining temporal variation in soil CO 2 efflux in a mature spruce forest in Southern Germany, Soil Biol. Biochem., 35(11), 1467–1483, 2003.

Suleau, M., Moureaux, C., Dufranne, D., Buysse, P., Bodson, B., Destain, J.-P., Heinesch, B., Debacq, A. and Aubinet, M.: Respiration of three Belgian crops: partitioning of total ecosystem respiration in its heterotrophic, above-and below-ground autotrophic components, Agric. For. Meteorol., 151(5), 633–643, 2011.

Van Oijen, M., Rougier, J. and Smith, R.: Bayesian calibration of process-based forest models: bridging the gap between models and data, Tree Physiol., 25(7), 915–927, 2005.

Vrugt, J. A.: Markov chain Monte Carlo simulation using the DREAM software package: Theory, concepts, and MATLAB implementation, Environ. Model. Softw., 75, 273–316, 2016.

Wang, G. and Chen, S.: A review on parameterization and uncertainty in modeling greenhouse gas emissions from soil, Geoderma, 170, 206–216, doi:10.1016/j.geoderma.2011.11.009, 2012.

5   Wang, Y.-P., Trudinger, C. M. and Enting, I. G.: A review of applications of model–data fusion to studies of terrestrial carbon fluxes at different scales, Agric. For. Meteorol., 149(11), 1829–1842, 2009.

Waring, R. H., Landsberg, J. J. and Williams, M.: Net primary production of forests: a constant fraction of gross primary production?, Tree Physiol., 18(2), 129–134, 1998.

Wlotzka, M., Haas, E., Kraft, P., Heuveline, V., Klatt, S., Kraus, D., Butterbach-Bahl, K. and Breuer, L.: Dynamic Simulation
10 of Land Management Effects on Soil N2O Emissions using a coupled Hydrology-Ecosystem Model, Prepr. Ser. Eng. Math. Comput. Lab, (03), 2013.

Wohlfahrt, G., Bahn, M., Haslwanter, A., Newesely, C. and Cernusca, A.: Estimation of daytime ecosystem respiration to determine gross primary production of a mountain meadow, Agric. For. Meteorol., 130(1), 13–25, 2005a.

Wohlfahrt, G., Anfang, C., Bahn, M., Haslwanter, A., Newesely, C., Schmitt, M., Drösler, M., Pfadenhauer, J. and Cernusca,
15 A.: Quantifying nighttime ecosystem respiration of a meadow using eddy covariance, chambers and modelling, Agric. For. Meteorol., 128(3), 141–162, 2005b.

Xiang, S.-R., Doyle, A., Holden, P. A. and Schimel, J. P.: Drying and rewetting effects on C and N mineralization and microbial activity in surface and subsurface California grassland soils, Soil Biol. Biochem., 40(9), 2281–2289, 2008.